

NOTES AND CORRESPONDENCE

**Future Projections in Precipitation over Asia Simulated by Two RCMs
Nested into MRI-CGCM2.2****Izuru TAKAYABU***Meteorological Research Institute, Tsukuba, Japan***Hisashi KATO, Keiichi NISHIZAWA***Central Research Institute of Electric Power Industry, Tokyo, Japan***Yukari N. TAKAYABU***Central of Climate System Research, University of Tokyo, Kashiwa, Japan***Yasuo SATO, Hidetaka SASAKI, Kazuo KURIHARA, and Akio KITO***Meteorological Research Institute, Tsukuba, Japan**(Manuscript received 31 May 2005, in final form 10 March 2007)***Abstract**

We statistically analyzed both the reproducibility of the present climate, and future climate projections in the Asian monsoon region, using two Regional Climate Models (RCMs), nested into the MRI-CGCM2.2 to assess regional climate projections associated with global warming. Both GCM-RCM systems reproduced the present regional surface air temperature well. Also, they indicated about the same temperature increases as that of GCM for all regions over the Asian continent. The reproducibility of the present-climate precipitation amounts, in the lower-latitude regions was not as good as that of the surface air temperature, although it was better simulated in the higher-latitude regions. The future precipitation increase was not statistically significant. It was also statistically revealed that precipitation in future projections, with GCM-RCM systems, tended to converge in regions where the model biases were small. This result suggests the importance of an accurate reproduction of the present regional climate using physically based dynamical models, in order to analyze regional climate changes.

1. Introduction

Regional-scale temperature, and precipitation changes associated with global warming, would greatly impact our lives. However, in

most cases, the horizontal resolution of general circulation models (GCMs) is insufficient to assess regional-scale climate change. Therefore, high-resolution regional climate models (RCMs), nested into GCMs are often utilized for regional-scale climate change studies. Hereafter, this paper will refer to such model systems as GCM-RCM nested modeling systems. Many studies have confirmed that regional precipitation patterns are better reproduced with

Corresponding author: Izuru Takayabu, Meteorological Research Institute, 1-1 Nagamine, Tsukuba Ibaraki 305-0052, Japan.
E-mail: takayabu@mri-jma.go.jp
© 2007, Meteorological Society of Japan

this approach (e.g., Bhaskaran et al. 1996; Jones et al. 1997; Nobre et al. 2001; Noda 2004), primarily because of superior representation of the orographic precipitation (e.g., Giorgi and Means 1991). However, previous works mostly discussed patterns of climate change, and did not reveal statistical approaches. Previous works that reveal statistical approaches are limited, but Giorgi et al. (2004) tried statistical analysis over the European region.

Some intercomparison studies used reanalysis data as the lateral boundary condition. Christensen et al. (1997), used seven RCMs with reanalysis data as boundary conditions, and simulated the present climate of Europe. They found that both local-, and global-scale phenomena influenced the reproducibility of surface temperature, and precipitation amount. These influences resulted from deficiencies in land surface schemes and radiation codes, biases in the activity of extratropical cyclones, and the difference in the mean sea level pressure (MSLP) patterns. However, they analyzed only two months' data out of one year, or two months' integrations, so that statistical conclusions were not derived. More recently, Fu et al. (2005) made an inter-comparison of regional climate models for Asia, using reanalysis data as the boundary condition.

It has been reported that the climate reproducibility of RCMs in present-climate simulations improves with the use of the reanalysis data, as the boundary condition instead of the GCM results (e.g., Seth and Rojas 2003; Rojas and Seth 2003). However, for future projection of the regional climate using RCMs, the GCM results are used as the boundary condition.

In this study, the aim is to clarify the statistical tendency in future projections of regional climate, utilizing nested RCMs and their relationship with present-climate reproducibility. Simulations are compared, by two different RCMs nested into a GCM. Both models have been used to perform future projection experiments, using the SRES A2 scenario (IPCC 2000). Results from the present climate (control run), and for the future climate (50 years of SRES A-2 scenario runs), are compared between the two. In this study, the models are integrated over ten years, which is much longer than Christensen et al. (1997) or Fu et al.

(2005), and then utilize the whole period of data for the statistics. The relation between model reproducibility of the present climate, and the results of future projection is discussed.

2. Models and experiments

In this study, the Central Research Institute of Electric Power Industry's RegCM3 (CRIEPI-RegCM3, hereafter referred to as C-R) is used, and the Meteorological Research Institute's Regional Climate Model (MRI-RCM, hereafter referred to as M-R), nested into the MRI-CGCM2.2 (Version 2.2 of the Meteorological Research Institute's atmosphere-ocean coupled general circulation model, Yukimoto et al. 2001; hereafter, we refer to this CGCM as M-G). RegCM3 is an improved version of the NCAR RegCM2 (Giorgi et al. 1993a,b), whose dynamical framework is the fourth-generation NCAR/Penn State Mesoscale Model (MM4; Anthes et al. 1987). As for the physics parameterization schemes, the radiation model of the Community Climate Model 3 (CCM3: Kiehl et al. 1996), and the Land Surface Model 1 (LSM1; Bonan 1996) are implemented in RegCM3. The dynamical framework of MRI-RCM is the Japan Meteorological Agency's Regional Spectral Model (JMA-RSM; the Numerical Prediction Division/JMA 1997). The grid size of these RCMs is 60 km, and they have 151×121 grid points (C-R), or 171×121 grid points (M-R).

The largest difference between the two RCMs concerning precipitation is their convection schemes: C-R uses the Kuo scheme (Anthes 1977), while M-R uses the prognostic Arakawa-Schubert (1974) scheme for cumulus convection, with its roots in the planetary boundary layers (Moorthi and Suarez 1992; Randall and Pan 1993). A moist convective adjustment scheme (Benwell and Bushby 1970; Gadd and Keers 1970) is added in M-R for middle-level convection (the Numerical Prediction Division/JMA 1997).

C-R and M-R are both directly nested into M-G. For both models, prognostic variables are nudged to the values given by M-G, within ten grids from the boundary. In the M-R, the spectral boundary coupling method proposed by Kida et al. (1991), and developed by Sasaki et al. (1995, 2000) was additionally used for levels above the altitude of 500 hPa. Ten-year runs of the present climate and future (50 years

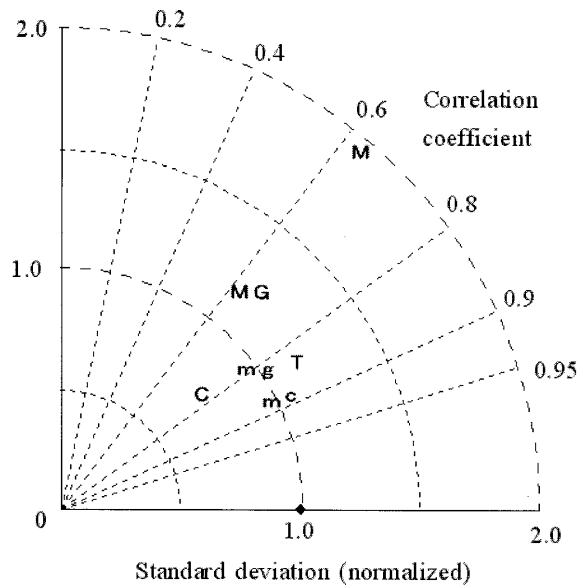


Fig. 1. Taylor diagram (Taylor, 2001) for the annual mean surface air temperature versus ERA (European Centre of Medium-Range Weather Forecast Re-Analysis) -15 data (lower-case letters), and the annual total precipitation of the models versus Global Precipitation Climatology Project (GPCP) data (capital letters). Area is 10° to 50°N and 70° to 140°E. C: C-R, M: M-R, MG: M-G. T indicates TRMM-PR2A25 data vs. GPCP data, for area 10° to 35°N and 70°E to 140°E.

ahead) projections, nested into the SRES A2 scenario runs of GCMs were performed.

In the following analysis, all nudged regions were removed from the analysis area.

3. Present climate

Figure 1 presents a Taylor diagram (Taylor 2001) covering the area of 10° to 50°N and 80° to 140°E. Here the total standard deviation is plotted, normalized by the observed value (NSD), and the correlation coefficients between the two fields (COR), for the simulated annual mean surface air temperature, against ERA-15's 2.5° × 2.5° grid data (Gibson et al. 1997), averaged over ten years (1981 to 1990), and those for the simulated annual precipitation amounts against GPCP (Global Precipitation Climatology Projection) 2.5° × 2.5° grid climate values (averaged from 1979 to 2005) (Adler

et al. 2003). All models' grid values are interpolated into the GPCP 2.5° × 2.5° grid. The reproducibility of the surface air temperature was good, with values of COR = 0.8–0.9, and NSD = 1 for the MRI-CGCM and two RCMs. However, the reproducibility of the precipitation amount varied among the models. Each model exhibited a correlation coefficient from 0.6 to 0.8, with the GPCP observation data. The percentage differences in simulated standard deviations to the observed one were +20% for the M-G, and -30% and +90% in the RCMs. Larger variations were evident in the standard deviation of precipitation between the two RCMs, compared to the MRI-CGCM, although the precipitation estimate of the GPCP tended to be too smooth in spatial variability, compared to the Tropical Rainfall Measuring Mission (TRMM) (indicated with T). It is generally accepted that the reproducibility of the precipitation amount is not as good as that of the surface air temperature of AOGCMs (IPCC TAR 2001). A GCM-RCM nested modeling systems in our study clearly had a similar tendency.

Next, how the models reproduced the present regional climate was examined. For this purpose, the Asian region into seven sub-regions (Fig. 2) was divided. Generally, temperature differences between model results and ERA-15 (1981–1990) were small for southern regions (#1, #2, #4, and #5), while decreases in reproducibility were found for high-latitude or inland regions (#3, #6, and #7) (not shown). However, the variation of the annual total precipitation was larger for the low-latitude regions (#1 and #2) and for the Tibetan Plateau (#3) (not shown). In the low-latitude regions, the bias in the simulated precipitation amount against GPCP became larger in RCMs, compared to their mother GCM, due to the convective schemes utilized in RCMs.

The precipitation over the ocean at low latitudes, was compared by comparing the histogram of the daily precipitation amount with the TRMM-3B42RT data. The TRMM data was smoothed into 0.5 × 0.5 grids, for direct comparison with 60 km grid model data. Figure 3 depicts precipitation histograms only for oceanic grid points within the area of 80°–140°E, 10°–25°N, binned with daily precipitation amounts. For the moderate (10 to 31.6 mm day⁻¹) to strong (31.6 to 100 mm day⁻¹) rain

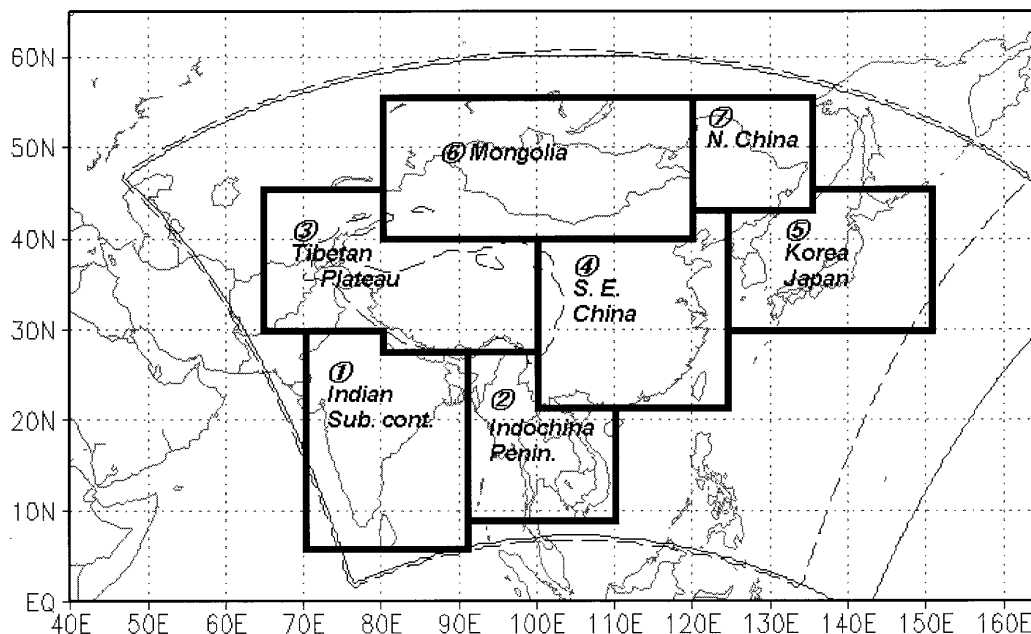


Fig. 2. Definition of regions used in this study. 1. Indian Sub-continent, 2. Indochina Peninsula, 3. Tibetan Plateau, 4. Southeast China region, 5. Korea-Japan region, 6. Mongolian region, and 7. North China region. The fan-shaped solid line indicates the area of M-R, and the broken line indicates the area of C-R. The thick broken line indicates 3000 m AGL.

bins, the precipitation amount was overestimated in M-R and underestimated in C-R. Over half of the precipitation came from the convective precipitation in this region (58% in C-R, and 88% in M-R). As shown in Fig. 4, both at high latitudes and over the land, C-R had the same precipitation pattern as the TRMM observation data. However, M-R underestimated the precipitation over land. Because C-R, and M-R were nested into the same GCM, it was suggested that the difference in physics schemes, resulted in large differences in precipitation amount.

Around the Tibetan Plateau (#3), all GCMs and RCMs exhibited large positive biases, in precipitation compared to GPCP. It is well known that the influence of the horizontal resolution on the orographic precipitation is very large around the Tibetan Plateau, and the low-resolution (T42) GCMs tend to overestimate precipitation along the southern periphery of the Tibetan Plateau. Kobayashi and Sugi (2004) demonstrated that increasing the horizontal resolution can alleviate this deficiency.

In all RCMs, the precipitation peak around

the southern periphery of the plateau appeared sharper than that of GCM (Fig. 4). A sharper precipitation maximum in this region was also distinct in TRMM 3B42RT data, while it was not as clear in GPCP. In C-R, another precipitation peak appeared at the northern edge of the plateau around 37° to 38°N, but it was not found in GPCP or in the TRMM data. The precipitation pattern in M-R was patchy compared to that of the TRMM. The low COR of RCM precipitation, with the GPCP was partly due to the fake peaks in the northern periphery of the Plateau of C-R, and partly due to the too-smooth distribution of the GPCP precipitation, because of its coarse resolution.

The predicted precipitation amount of the RCMs, exhibited better agreement with the GPCP in higher-latitude regions (#4 to #7). Particularly in C-R, the difference between the model simulated values, and the GPCP values, was within one standard deviation.

4. SRES A2 scenario runs

In this section, future projections in surface air temperature was compared and precipita-

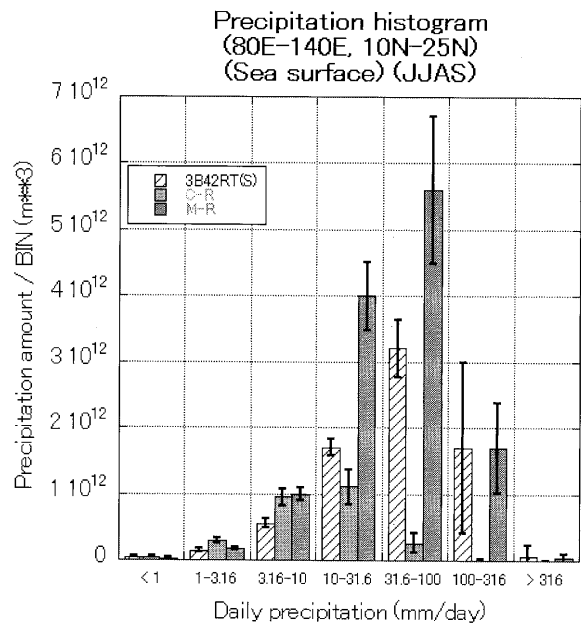


Fig. 3. Histogram of daily precipitation amounts binned to 0–1.0, 1.0–3.16, 3.16–10.0, 10.0–31.6, 31.6–100, 100–316, and >316 mm day⁻¹ for (a) TRMM3B42RT, (b) C-R, and (c) M-R (bar graphs from left to right), obtained from the ocean grids of 80°E–140°E and 10°N–30°N. The ordinate is the precipitation amount per BIN. The 95% *t*-test intervals are also drawn.

tion between the two GCM-RCM nested modeling systems. Figure 5a compares the annual mean surface air temperature change in the next 50 years (from 2046 to 2055). The temperature increases for all seven regions with all the RCMs. Both RCMs have about the same temperature increase as that of their mother GCMs.

Figure 5b indicates the changes in the area's average annual precipitation amounts. Similar to the surface air temperature, the total precipitation mostly increases, except in region #2. However, the statistics indicate that the increase is significant in only the higher-latitude regions (#3, #6, and #7) in C-R or M-R. These results suggest that the precipitation amount will increase in the next 50 years, but the signal is still not significant. It is beyond the scope of this paper to estimate the influence of the

decadal oscillation, because we integrate only for 10 years long. If a linear trend is assumed, with time and no change in the 95% confidence interval, the signal would become significant within 60 to 70 years from now in the C-R or the M-R. In contrast, when the same hypothesis is adopted with the surface air temperature, the temperature increase would become significant ten years from now.

5. Relationship between the present-climate simulations and the future projections of precipitation

In the previous sections, the reproducibility of the present climate was examined, and future projections of the RCMs were examined separately. Here, we examine the relationship between the reproducibility of the present climate and the future projection. For this purpose, we compared the “reproducibility” of the precipitation patterns of the current climate and the “convergence” of the future projections. While a true validation for the future projection is not possible, convergence of results from different models can be one of the measures of reliability in projections.

As for the “reproducibility” index (Index-P), we calculated a normalized square root variance of precipitation against the GPCP estimates for two models in the area of 80–140 E, 10–55 N from June through September, as follows:

$$IndexP = \frac{1}{GPCP} \sqrt{\frac{\sum_{m=1}^M \sum_{i=1}^N (x_{im} - GPCP_i)^2}{MN - 1}}, \quad (1)$$

where x_{im} is the precipitation amount at grid number i of model number m , M is the number of models to compare, and N is the number of grids in the comparison area. We smoothed all RCM grid values into the GPCP's $2.5^\circ \times 2.5^\circ$ grid. $GPCP_i$ is the precipitation amount of GPCP at grid number i , and $\overline{GPCP} = \frac{1}{N} \sum_{i=1}^N GPCP_i$. However, in order to represent the “convergence” of future projections (Index-F), we calculated a normalized square root variance of two RCMs against the model average, as follows:

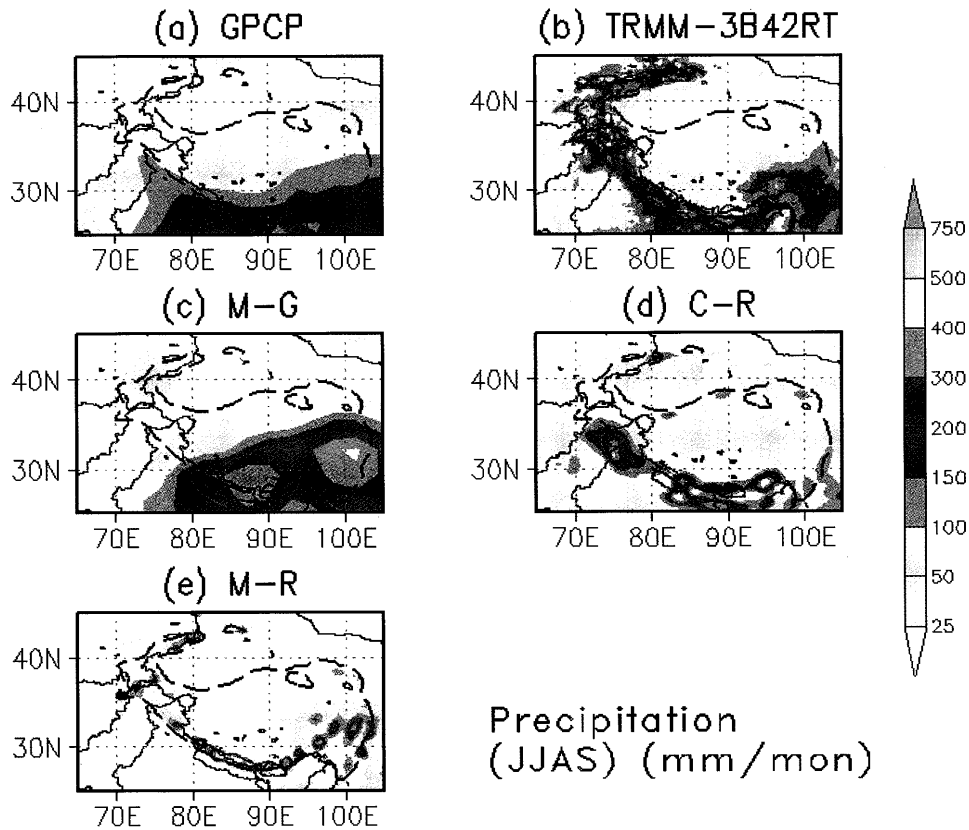


Fig. 4. Precipitation amount around the Tibetan Plateau for JJAS of (a) GPCP 2.5 degrees data, (b) TRMM-3B42RT 0.25 degrees data (2002–2004), (c) M-G, (d) C-R, and (e) M-R. The thick broken line denotes 3000 m AGL.

$$IndexF = \frac{1}{\bar{x}} \sqrt{\frac{\sum_{m=1}^M \sum_{i=1}^N (x_{im} - \bar{x}_i)^2}{MN - 1}}, \quad (2)$$

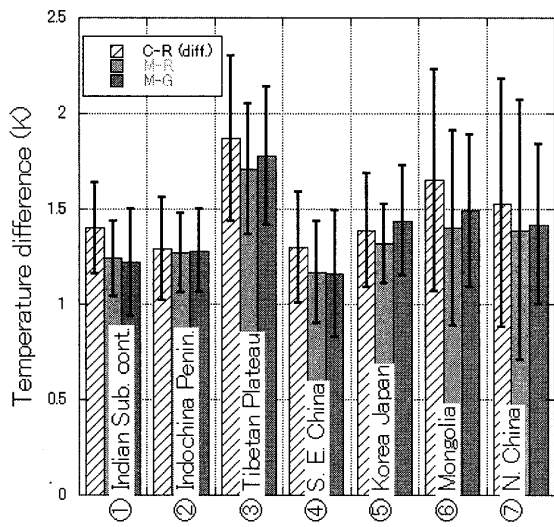
where x_{im} is the future precipitation amount at grid point i , $\bar{x}_i = \frac{1}{M} \sum_{m=1}^M x_{im}$ and $\bar{x} = \frac{1}{N} \sum_{i=1}^N \bar{x}_i$. Here we divided the whole area (80° to 140°E, 10° to 55°N) into 36 rectangular regions (10.0° × 7.5°), and made a scatter diagram of Indices-P against Indices-F (Fig. 6). A significant positive correlation between Indices-P and Indices-F (correlation coefficient of 0.73) strongly indicated that where the reproducibility of the current precipitation distribution was high, the future projections tended to converge. Both Index-F and Index-P had smaller values in higher latitudes than in lower latitudes. Note that the variance of the precipitation also represents the characteristics of the precipita-

tion. Therefore, the correlation between Index-F and Index-P provides information on the future predictability of precipitation depending on both precipitation characteristics and inter-model convergence.

6. Conclusions

Two RCMs with a horizontal resolution of 60 km, nested into a GCM with a horizontal resolution of 280 km, were utilized to reproduce the regional climate at the end of the 20th century and to project the future climate in the 2050s with the SRES A2 scenario. The RCMs covered the Asian monsoon region, including the Indian subcontinent, Tibetan plateau, Indochina Peninsula, China, and the Korea-Japan region. Both RCMs represented the surface air temperature well. In addition, they indicated large annual temperature increases for all seven sub-regions over the Asian continent. The reproducibility of the precipitation amount

(a) Temperature difference (future - present)



(b) Precipitation amount difference (future - present)

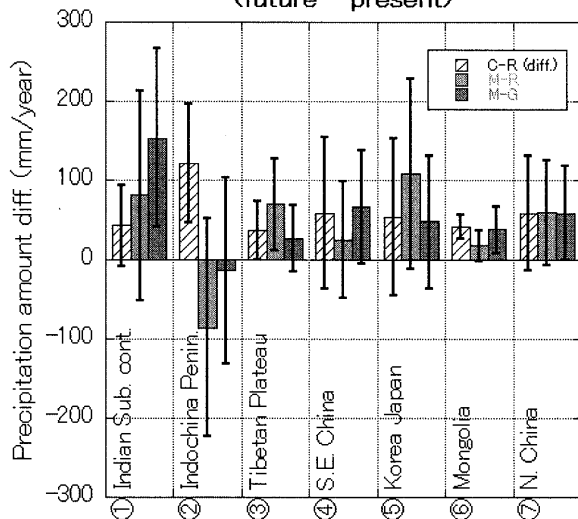


Fig. 5. The differences of (a) the annual mean surface air temperature and (b) total precipitation simulated by C-R, M-R, and M-G. The 95% *t*-test intervals of the difference between future and present are also drawn for seven regions, as indicated in Fig. 2.

was not as good as that of the surface air temperature for lower-latitude regions. However, the precipitation amount indicated better reproducibility in the higher-latitude regions. The precipitation increase 50 years from now,

Reproducibility & Projection

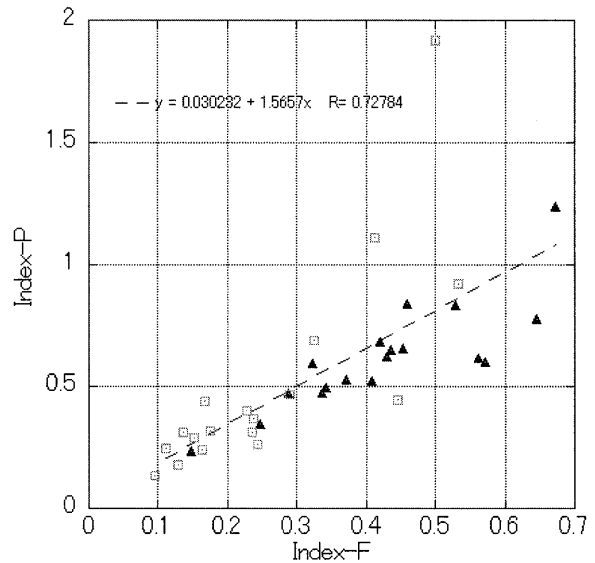


Fig. 6. Scatter diagram of Index-F against Index-P for monthly total precipitation of the mean value of June to September (JJAS). Triangles (10° – 32.5° N) and rectangles (32.5° – 55° N) indicate values of 36 rectangular regions ($10.0^{\circ} \times 7.5^{\circ}$) within the whole area (80° – 140° E, 10° – 55° N).

was not as significant as that of the surface air temperature. Detailed examinations of the RCM precipitation, revealed that future projections tended to converge in regions where the model biases were small. This result suggested the importance of the accurate reproduction of the present regional climate, using physically based dynamical models, in order to analyze regional climate changes. Undeniably, the same trend in different models could result from different causes, which is a possibility left for future studies.

Acknowledgements

The authors express their gratitude to Prof. J. G. Huffman of NASA GSFC for his valuable advice on the TRMM 3B42RT data. The GPCP data used in this paper was prepared by NASA GSFC, and the ERA-15 data was prepared by ECMWF (ECMWF, 1996: The Description of the ECMWF Re-analysis Global Atmospheric Data Archive). The authors are also grateful to Dr. S. Emori, Dr. T. Nozawa of NIES, and Dr.

K. Dairaku of NIED for their many helpful comments. They are also much obliged to the anonymous referees for reading the manuscripts and giving valuable comments. Part of this study was supported by "Water Resources and Variability in Asia in the 21st Century" of MEXT, and also by the Climate Change Prediction Fund of the Japan Meteorological Agency.

References

- Adler, R.F., G.J. Huffman, A. Chang, R. Ferraro, P.-P. Xie, J. Janowiak, B. Rudolf, U. Schneider, S. Curtis, D. Bolvin, A. Gruber, J. Susskind, P. Arkin, and E. Nelkin, 2003: The version-2 Global Precipitation Climatology Project (GPCP) Monthly Precipitation Analysis (1979-Present). *J. Hydrometeor.*, **4**, 1147–1167.
- Anthes, R.A., 1977: A cumulus parameterization scheme utilizing a one-dimensional cloud model. *Mon. Wea. Rev.*, **105**, 270–286.
- Anthes, R.A., E.-Y. Hsie, and Y.-H. Kuo, 1987: Description of the Penn State/NCAR Mesoscale Model version 4 (MM4). *NCAR Technical Note*. NCAR/TN-282+STR, 66 pp.
- Arakawa, A. and W.H. Schubert, 1974: Interactions of cumulus cloud ensemble with the large-scale environment. Part I. *J. Atmos. Sci.*, **31**, 671–701.
- Benwell, G.R.R. and F.H. Bushby, 1970: A case study of frontal behavior using a 10-level primitive equation model. *Quart. J. Roy. Meteor. Soc.*, **96**, 287–296.
- Bhaskaran, B., R.G. Jones, J.M. Murphy, and M. Noguer, 1996: Simulations of the Indian summer monsoon using a nested regional climate model: domain size experiments. *Clim. Dyn.*, **12**, 573–587.
- Bonan, G.B., 1996: The NCAR land surface model (LSM version 1.0) coupled to the NCAR Community Climate Model. *NCAR Technical Note*, NCAR/TN-282+STR, 66 pp.
- Christensen, J.H., B. Machenhauer, R.G. Jones, C. Schaer, P.M. Ruti, M. Castro, and G. Visconti, 1997: Validation of present-day regional climate simulations over Europe: LAM simulations with observed boundary conditions. *Clim. Dyn.*, **13**, 489–506.
- Fu, C., S. Wang, Z. Xiong, W.J. Gutowski, D.-K. Lee, J.L. McGregor, Y. Sato, H. Kato, J.-W. Kim, and M.-S. Suh, 2005: Regional climate model inter-comparison project for Asia. *Bull. Amer. Meteor. Soc.*, **86**, 257–266.
- Gadd, A.J. and J.F. Keers, 1970: Surface exchanges of sensible and latent heat in a 10-level model atmosphere. *Quart. J. Roy. Meteor. Soc.*, **96**, 297–308.
- Gibson, J.K., P. Kallberg, S. Uppala, A. Hernandez, A. Nomura, and E. Serrano, 1997: ERA description. ECMWF Re-Analysis Preproject Report Series, **1**, 72 pp.
- Giorgi, F. and L.O. Means, 1991: Approaches to the simulation of regional climate change: A review. *Rev. Geophysics*, **29**, 191–216.
- Giorgi, F., M.R. Marinucci, and G.T. Bates, 1993a: Development of a second-generation regional climate model (RegCM2) I: Boundary layer and radiative transfer processes. *Mon. Wea. Rev.*, **121**, 2794–2813.
- Giorgi, F., M.R. Marinucci, G.T. Bates, and G. De Canio, 1993b: Development of a second-generation regional climate model (RegCM2) II: Convective processes and assimilation of lateral boundary conditions. *Mon. Wea. Rev.*, **121**, 2814–2832.
- Giorgi, F., X. Bi, and J. Pal, 2004: Mean, interannual variability and trends in a regional climate change experiment over Europe. II: climate change scenarios (2071–2100). *Clim. Dyn.*, **23**, 839–858.
- Iguchi, T., T. Kozu, R. Meneghini, J. Arakawa, and K. Okamoto, 2000: Rain-profiling algorithm for the TRMM precipitation radar. *J. Appl. Meteor.*, **39**, 2038–2052.
- IPCC, 2000: Special Report on Emission Scenarios. A Special Report of Working Group III of the Intergovernmental Panel on Climate Change. [Nakicenovic, N., J. Aleamo, G. Davis, B. de Vries, J. Fenhann, S. Gaffin, K. Gregory, A. Grüber, T. Yong Jung, T. Kram, E.L. La Rovere, L. Michaelis, S. Mori, T. Morita, W. Pepper, H. Pitcher, L. Price, K. Riahi, A. Roehrl, H.-H. Rogner, A. Sankovski, M. Schlesinger, P. Shukla, S. Smith, R. Swart, S. van Rooijen, N. Victor, and Z. Dadi (eds.)]. Cambridge University Press, Cambridge, UK.
- IPCC, 2001: *Climate Change 2001: The Scientific Basis. Contribution of Working Group I to the Third Assessment Report of the Intergovernmental Panel on Climate Change* [Houghton, J.T., Y. Ding, D.J. Griggs, M. Noguer, P.J. van der Linden, X. Dai, K. Maskell, and C.A. Johnson (eds.)]. Cambridge University Press, Cambridge, United Kingdom and New York, NY, USA, 881 pp.
- Jones, R.G., J.M. Murphy, M. Noguer, and A.B. Keen, 1997: Simulation of climate change over Europe using a nested regional-climate model. II: Comparison of drivind and regional model responses to a doubling of carbon dioxide. *Quart. J. Roy. Meteor. Soc.*, **123**, 265–292.
- Kida, H., T. Koide, H. Sasaki, and M. Chiba, 1991: A new approach for coupling a limited area model to a GCM for regional climate

- simulations. *J. Meteor. Soc. Japan*, **69**, 723–728.
- Kiehl, J.T., J.J. Hack, G.B. Bonan, B.A. Boville, B.P. Briegleb, D.L. Williamson, and P.J. Rasch, 1996: Description of the NCAR Community Climate Model (CCM3). *NCAR Technical Note*, NCAR/TN-420+STR, 152 pp.
- Kobayashi, C. and M. Sugi, 2004: Impact of horizontal resolution on the simulation of the Asian summer monsoon and tropical cyclones in the JMA global model. *Clim. Dyn.*, **93**, 165–176.
- Moorthi, S. and M.J. Suarez, 1992: Relaxed Arakawa-Schubert: A parameterization of moist convection for general circulation models. *Mon. Wea. Rev.*, **120**, 978–1002.
- Nobre, P., A.D. Moura, and L. Sun, 2001: Dynamical downscaling of seasonal climate prediction over nordeste Brazil with ECHAM3 and NCEP's regional spectral models at IRI. *Bull. Amer. Meteor. Soc.*, **82**, 2787–2796.
- Noda, A., 2004: Research on global warming projection by regional climate models, in Global warming—The research challenges—A report of Japan's global warming initiative, A. Ichikawa Ed., Springer verlag.
- Numerical Prediction Division/JMA, 1997: Outline of the operational numerical weather prediction at the Japan Meteorological Agency, Appendix to Progress Report on Numerical Weather Prediction.
- Randall, D.A. and D.-M. Pan, 1993: Implementation of the Arakawa-Schubert cumulus parameterization with a prognostic closure. Meteorological Monograph/The representation of cumulus convection in numerical models. *J. Atmos. Sci.*, **46**, 137–144.
- Rojas, M. and A. Seth, 2003: Simulation and sensitivity in a nested modeling system for South America. Part II: GCM boundary forcing. *J. Climate*, **16**, 2454–2471.
- Sasaki, H., H. Kida, T. Koide, and M. Chiba, 1995: The performance of long-term integrations of a limited area model with the spectral boundary coupling method. *J. Meteor. Soc. Japan*, **73**, 165–181.
- Sasaki, H., Y. Sato, K. Adachi, and H. Kida, 2000: Performance and evaluation of the MRI regional climate model with the spectral boundary coupling method. *J. Meteor. Soc. Japan*, **78**, 477–489.
- Seth, A. and M. Rojas, 2003: Simulation and sensitivity in a nested modeling system for South America. Part I: Reanalysis boundary forcing. *J. Climate*, **16**, 2437–2453.
- Taylor, K.E., 2001: Summarizing multiple aspects of model performance in a single diagram, *J. Geophys. Res.*, **106**, D7, 7183–7192.
- Yukimoto, S., A. Noda, A. Kitoh, M. Sugi, Y. Kitamura, M. Hosaka, K. Shibata, S. Maeda, and T. Uchiyama, 2001: The new Meteorological Research Institute coupled GCM (MRI-CGCM2)—Model climate and variability—. *Pap. Meteor. Geophys.*, **51**, 47–88.